Computers and Mathematics with Applications 62 (2011) 2169–2176

Contents lists available at SciVerse ScienceDirect

Computers and Mathematics with Applications

journal homepage: www.elsevier.com/locate/camwa

Thermodynamic modeling of performance of a Miller cycle with engine speed and variable specific heat ratio of working fluid

Rahim Ebrahimi *

Department of Agriculture Machine Mechanics, Shahrekord University, P.O. Box 115, Shahrekord, Iran

ARTICLE INFO

Article history:
Received 12 February 2011
Received in revised form 5 July 2011
Accepted 5 July 2011

Keywords:
Miller heat-engine
Finite-time processes
Heat resistance
Friction
Internal irreversibility

ABSTRACT

The performance of an air standard Miller cycle is analyzed using finite-time thermodynamics. The results show that if the compression ratio is less than certain value, the increase of the value of the specific heat ratio will make the power output bigger. In contrast, if the compression ratio exceeds certain value, the increase of the value of the specific heat ratio will make the power output less. The results also show that if the compression ratio is less than certain value, the power output decreases with increasing engine speed, while if the compression ratio exceeds certain value, the power output first increases and then starts to decrease with increasing engine speed. With a further increase in compression ratio, the increase of engine speed results in decreasing the power output. The results are of importance to provide good guidance for the performance evaluation and improvement of practical Miller engines.

© 2011 Elsevier Ltd. All rights reserved.

1. Introduction

A series of achievements have been made since finite-time thermodynamics was used to analyze and optimize the performance of real thermodynamic processes, devices and cycles [1–5]. In the 1940's, Miller [6] proposed a different Otto cycle with an unequal compression and expansion stroke called the Miller cycle. The Miller cycle has been given attention recently [7], and some authors have examined the finite-time thermodynamic performance of the Miller cycle. Hatamura et al. [8] reported that the Miller cycle has advantages such as a higher mean effective pressure than the Otto cycle with lower nominal compression ratio. Fukuzawa et al. [9] described the main technologies and performance specifications for a high efficiency Miller cycle gas engine as well as for the series of engines planned in the future. Al-Sarkhi et al. [10] compared the performance characteristic curves of the Atkinson cycle with those of the Miller and Joule–Brayton cycles by using numerical examples, and outlined the effect of maximizing power density on the performance of the cycle efficiency. Sasaki et al. [11] reported an efficient Miller cycle with a high performance capacitor system for hybrid busses. Wu et al. [12] performed a performance analysis and optimization of a supercharged Miller cycle Otto engine. Ge et al. derived the performance characteristics of the Miller cycle with heat transfer loss [13] and with heat transfer and friction-like term losses [14] respectively. These works were done without considering the variable specific heats of the working fluid. Ge et al. [15] also studied the effect of variable specific heats of working fluid on the performance of an endoreversible Miller cycle. Al-Sarkhi et al. [16] and Zhao and Chen [17] presented theoretical investigations into the Miller cycle's engine performance, studying the influence of the main engine design variables and system irreversibilities. Al-Sarkhi et al. [18] evaluated the performance of the Miller engine by taking into consideration the different specific heat models (i.e., constant, linear, and fourth order

* Tel.: +98 3814424428; fax: +98 3814424428.
E-mail addresses: Rahim.Ebrahimi@gmail.com, Ebrahimi-r@agr.sku.ac.ir.

0898-1221/$ – see front matter © 2011 Elsevier Ltd. All rights reserved.
doi:10.1016/j.camwa.2011.07.002

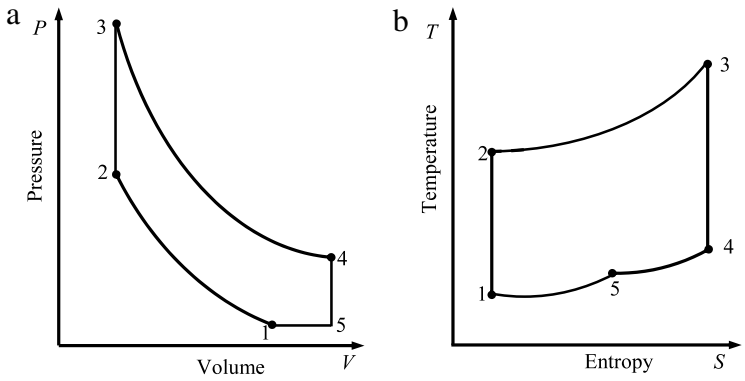

Fig. 1. (a) P–V diagram; (b) T–S diagram for the air standard Miller cycle.

polynomial). It was found that an accurate model such as the fourth order polynomial is essential for accurate prediction of cycle performance. Lin and Hou [19] examined the effects of heat loss characterized by a percentage of fuel energy, friction and variable specific heats of working fluid on the performance of an air standard Miller cycle under the restriction of maximum cycle temperature. Chen et al. [20] built a class of generalized irreversible universal steady flow heat engine cycle model consisting of two heating branches, two cooling branches, and two adiabatic branches considering the losses of heat resistance, heat leakage, and internal irreversibility. The performance characteristics of Diesel, Otto, Brayton, Atkinson, dual and Miller cycles were derived. Liu and Chen [21] established a general irreversible cycle model of a class of typical heat engines by considering variable heat capacities of the working fluid, irreversibility resulting from the compression and expansion processes and heat leak losses.

In all of the above mentioned researches, the specific heats at a constant pressure and volume of working fluid are assumed to be constants or functions of temperature alone and have linear or the nonlinear forms. But when calculating the chemical heat released in combustion at each instant of time for internal combustion engine, the specific heat ratio is generally modeled as a linear function of mean charge temperature [22]. The model has been used and the phenomena that it takes into account are well known [23]. However, since the specific heat ratio has a great influence on the heat release peak and on the shape of the heat release curve [24], some researchers have elaborated different mathematical equations to describe the dependence of specific heat ratio on temperature [22–25]. It should be mentioned here that the most important thermodynamic property used in the heat release calculations for engines is the specific heat ratio [25]. It should be also noted that the value of specific heat ratio of inlet charge can be varied by changing the rate of exhaust gas recirculation (EGR) in real engines. EGR is a common way to control in-cylinder nitric oxide production and is used on most modern internal combustion engines [26]. Also, the investigation of the effect of engine speed on the performance of the Miller cycle does not appear to have been published. Therefore, the objective of this study is to examine the effect of variable specific heat ratio and engine speed on the power output and the thermal efficiency of the air standard Miller cycle.

2. Cycle analysis

The pressure–volume (P–V) and the temperature–entropy (T–S) diagrams of an irreversible Miller heat engine is shown in Fig. 1, where T_1, T_2, T_3, T_4 and T_5 are the temperatures of the working fluid in state points 1, 2, 3, 4 and 5. Process $1 \rightarrow 2$ is an isentropic compression. The heat addition occurs in the constant volume process $2 \rightarrow 3$. The process $3 \rightarrow 4$ is an isentropic expansion process. Heat rejection occurs in two steps: processes $4 \rightarrow 5$ and $5 \rightarrow 1$ are constant volume and constant pressure heat rejections, respectively.

As already mentioned in the previous section, it can be supposed that the specific heat ratio of the working fluid is a function of temperature alone and has the linear forms:

$$\gamma = \gamma_\circ - k_1 T \tag{1}$$

where γ is the specific heat ratio and T is the absolute temperature. $\gamma_\circ$ and k_1 are constants.

Assuming that the heat engine is operated at the rate of N revolutions per second, the heat added per second in the isochoric $2 \rightarrow 3$ heat addition process may be written as:

$$Q_{in} = NM \int_{T_2}^{T_3} c_v \mathrm{d}T = NM \int_{T_2}^{T_3} \left(\frac{R}{\gamma_\circ - k_1 T - 1} \right) \mathrm{d}T = \frac{NMR}{k_1} \ln \left(\frac{\gamma_\circ - k_1 T_2 - 1}{\gamma_\circ - k_1 T_3 - 1} \right) \tag{2}$$

where M is the molar number of the working fluid. R and c_v are molar gas constant and molar specific heat at constant volume for the working fluid, respectively.

The heat rejected per second by the working fluid during processes $4 \to 5$ and $5 \to 1$ is

$$\begin{aligned} Q_{out} &= NM\left(\int_{T_5}^{T_4} c_v \mathrm{d}T + \int_{T_1}^{T_5} c_p \mathrm{d}T\right) \\ &= NM\left[\int_{T_5}^{T_4}\left(\frac{R}{\gamma_\circ - k_1 T - 1}\right)\mathrm{d}T + \int_{T_1}^{T_5}\left(\frac{(\gamma_\circ - k_1 T)\,R}{\gamma_\circ - k_1 T - 1}\right)\mathrm{d}T\right] \\ &= NMR\left[T_5 - T_1 + \frac{1}{k_1}\ln\left(\frac{\gamma_\circ - k_1 T_1 - 1}{\gamma_\circ - k_1 T_4 - 1}\right)\right] \end{aligned} \tag{3}$$

where c_p is the molar specific heat at constant pressure for the working fluid.

According to Refs. [15,27], the equation for a reversible adiabatic process with variable specific heat ratio can be written as follows:

$$TV^{\gamma-1} = (T + \mathrm{d}T)\,(V + \mathrm{d}V)^{\gamma-1}. \tag{4}$$

Re-arranging Eqs. (1) and (4), we get the following equation

$$T_i\left(\gamma_\circ - k_1 T_j - 1\right) = T_j\left(\gamma_\circ - k_1 T_i - 1\right)\left(V_j/V_i\right)^{\gamma_\circ - 1}. \tag{5}$$

The volume ratio of heat rejection process, ψ, the effective compression ratio, r_c^*, and the compression ratio, r_c, are defined as:

$$\psi = \frac{V_5}{V_1} = \frac{T_5}{T_1} \tag{6}$$

$$r_c^* = \frac{V_1}{V_2} \tag{7}$$

and

$$r_c = \frac{V_5}{V_2} = \psi r_c^*. \tag{8}$$

Therefore, the equations for processes $(1 \to 2)$ and $(3 \to 4)$ are shown, respectively, by the following:

$$T_1\left(\gamma_\circ - k_1 T_2 - 1\right)\left(r_c^*\right)^{\gamma_\circ - 1} = T_2\left(\gamma_\circ - k_1 T_1 - 1\right) \tag{9}$$

and

$$T_3\left(\gamma_\circ - k_1 T_4 - 1\right) = T_4\left(\gamma_\circ - k_1 T_3 - 1\right)\left(\psi r_c^*\right)^{\gamma_\circ - 1}. \tag{10}$$

For an ideal Miller cycle model, there are no losses. However, for a real internal combustion engine cycle, the heat transfer irreversibility between the working fluid, the cylinder wall and friction like term loss are not negligible. The heat loss through the cylinder wall is assumed to be proportional to the average temperature of both the working fluid and the cylinder wall and the wall temperature is constant. The energy transferred to the working fluid during combustion is given by the following linear relation [10,13,27].

$$Q_{in} = NM\left[A - B\left(T_2 + T_3\right)\right] \tag{11}$$

where A and B are two constants related to combustion and heat transfer which are functions of engine speed. From Eq. (11), it can be seen that Q_{in} contains two parts: the first part is NMA, the released heat by combustion per second, and the second part is the heat leakage loss per second, $Q_{leak} = NMB\left(T_2 + T_3\right)$.

Taking into account the friction loss of the piston and assuming a dissipation term represented by a friction force that is a linear function of the piston velocity gives [3,13]

$$f_\mu = -\mu v = -\mu\frac{\mathrm{d}x}{\mathrm{d}t} \tag{12}$$

where μ is the coefficient of friction, which takes into account the global losses, x is the piston's displacement and v is the piston's velocity. Therefore, the lost power due to friction is

$$P_\mu = \frac{\mathrm{d}W_\mu}{\mathrm{d}t} = -\mu\left(\frac{\mathrm{d}x}{\mathrm{d}t}\right)^2 = -\mu v^2. \tag{13}$$

Running at N revolutions per second, the mean velocity of the piston is [28]:

$$\bar{v} = 2LN = 2L^*\left[1 + \frac{r_c^*\left(\psi - 1\right)}{r_c^* - 1}\right]N \tag{14}$$

where L is the total distance the piston travels per cycle and L^* is the length of the isentropic process 1–2.

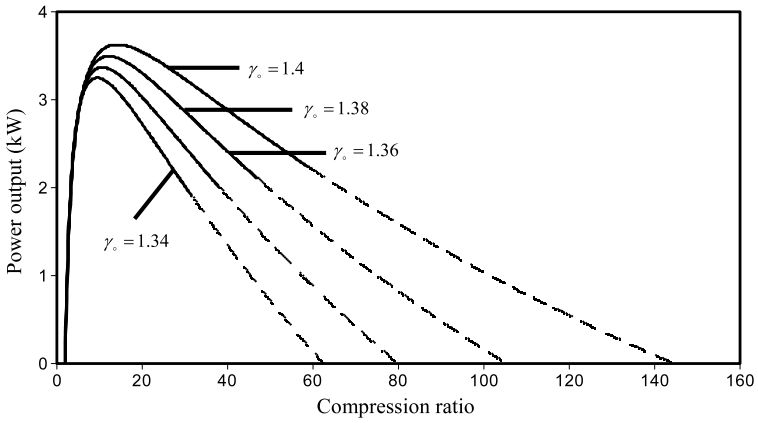

Fig. 2. Effect of $\gamma_\circ$ on the $P_{out} - r_c$ characteristic for $k_1 = 0.00008\ \mathrm{K}^{-1}$ and $N = 3000$ rpm.

From Eqs. (2), (3) and (13), the power output of the Miller cycle engine is given by:

$$P_{out} = \frac{W}{\tau} - P_\mu = \frac{NMR}{k_1} \ln\left(\frac{(\gamma_\circ - k_1T_2 - 1)(\gamma_\circ - k_1T_4 - 1)}{(\gamma_\circ - k_1T_3 - 1)(\gamma_\circ - k_1T_1 - 1)}\right) + NMR(T_1 - T_5) - 4\mu\left(L^*\left[1 + \frac{r_c^*(\psi - 1)}{r_c^* - 1}\right]N\right)^2. \tag{15}$$

The thermal efficiency of the Miller cycle engine is expressed by:

$$\eta_{th} = \frac{P_{out}}{Q_{in}} = \frac{\ln\left(\frac{(\gamma_\circ - k_1T_2 - 1)(\gamma_\circ - k_1T_4 - 1)}{(\gamma_\circ - k_1T_3 - 1)(\gamma_\circ - k_1T_1 - 1)}\right) + k_1NMR(T_1 - T_5) - \frac{4\mu k_1}{NMR}\left(L^*\left[1 + \frac{r_c^*(\psi - 1)}{r_c^* - 1}\right]N\right)^2}{\ln\left(\frac{\gamma_\circ - k_1T_2 - 1}{\gamma_\circ - k_1T_3 - 1}\right)}. \tag{16}$$

When r_c^*, ψ and T_1 are given, T_2 can be obtained from Eq. (9); then, substituting Eq. (2) into Eq. (11) yields T_3; and T_4 can be found from Eq. (10); at last, T_5 can be found by Eq. (6). Substituting T_1, T_2, T_3, T_4 and T_5 into Eqs. (15) and (16) yields the power output and thermal efficiency. Therefore, the relations between the power output, the thermal efficiency and the compression ratio can be derived.

3. Numerical examples and discussion

The following constants and parameters have been used in this exercise: $\psi = 1.3$, $T_1 = 280$ K, $B = 25\ \mathrm{J\ mol^{-1}\ K^{-1}}$, $A = 60\,000\ \mathrm{J\ mol^{-1}}$, $L^* = 70$ mm, $M = 0.00015 \times N \times L^*$ kmol, $\mu = 12.9\ \mathrm{N\,s\,m^{-1}}$, $k_1 = 0.00002 \rightarrow 0.0011\,K^{-1}$, $\gamma_\circ = 1.34 \rightarrow 1.4$ and $N = 1000 \rightarrow 7000$ rpm [8,10,15,29–32]. Using the above constants and ranges of parameters, the power output versus compression ratio characteristic and the power output versus thermal efficiency characteristic can be plotted as in Figs. 2–7 (the dashed lines in the figures denote where the cycle can not work on, when T_5 exceeds T_4).

Figs. 2–5 show the effects of the variable specific heat ratio of the working fluid on the performance of the cycle with heat resistance and friction irreversible losses. From these figures, it can be found that $\gamma_\circ$ and k_1 play a key role on the power output and the thermal efficiency. It is clearly seen that the effects of $\gamma_\circ$ and k_1 on the power output and thermal efficiency are related to the compression ratio. They reflect the performance characteristics of an irreversible Miller cycle engine. It should be mentioned here that for a fixed k_1, a larger $\gamma_\circ$ corresponds to a greater value of the specific heat ratio and for a given $\gamma_\circ$, a larger k_1 corresponds to a lower value of the specific heat ratio. k_1 reflects the degree of variation of the specific heat ratio with temperature.

The effects of $\gamma_\circ$ and k_1 on the power output are shown in Figs. 2 and 3. It can be found from these figures that the power output versus compression ratio characteristic produces approximately parabolic like curves. In other words, the power output increases with increasing compression ratio, reaches their maximum values and then decreases with the further increase in compression ratio. It can also be found from the Figs. 2 and 3 that if the compression ratio is less than a certain value, the increase (decrease) of $\gamma_\circ(k_1)$ will increase the power output, due to the increase in the difference between heat added and heat rejected. In contrast, if the compression ratio exceeds a certain value, the increase (decrease) of $\gamma_\circ(k_1)$ will reduce the power output, because of the decrease in the difference between heat added and heat rejected. One can see that the maximum power output, the range of r_c in which the cycle can work normally and the optimal compression

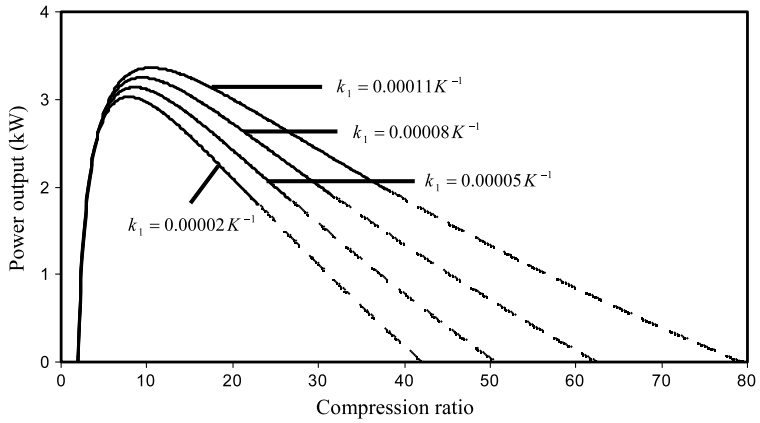

Fig. 3. Effect of k_1 on the $P_{out} - r_c$ characteristic for $\gamma_\circ = 1.4$ and $N = 3000$ rpm.

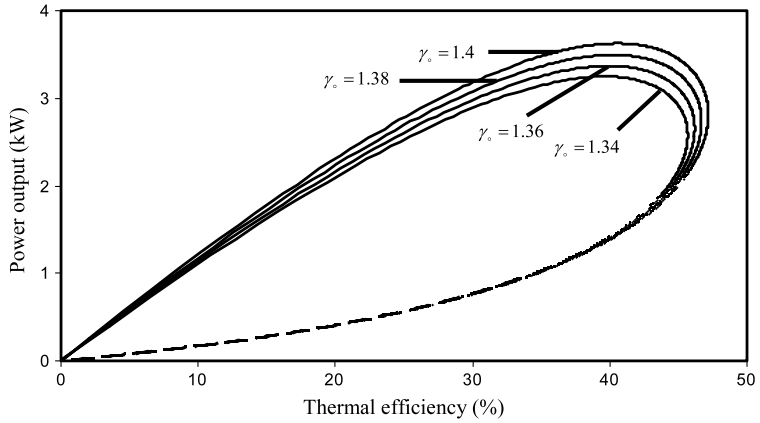

Fig. 4. Effect of $\gamma_\circ$ on the $\eta_{th} - r_c$ characteristic for $k_1 = 0.00008$ K^{-1} and $N = 3000$ rpm.

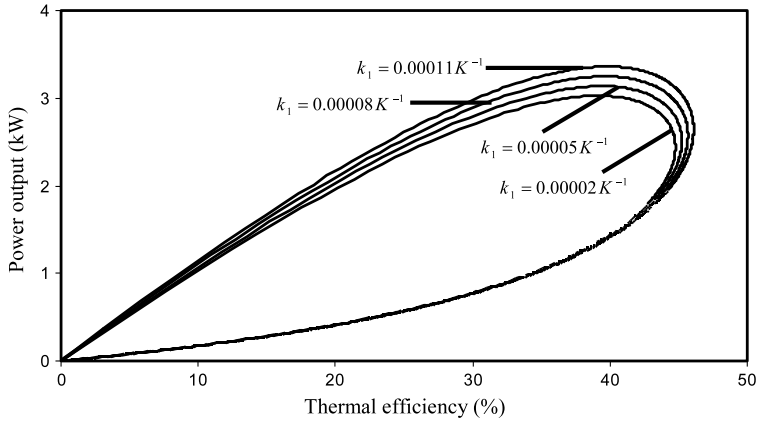

Fig. 5. Effect of k_1 on the $\eta_{th} - r_c$ characteristic for $\gamma_\circ = 1.4$ and $N = 3000$ rpm.

ratio corresponding to maximum power output decrease (increase) is about 10.4% (7.3%) and 47.5% (39.5%), 33% (19.7%), respectively, when $\gamma_\circ(k_1)$ increases (increases) 4.2% (81.9%). This is due to the fact that the difference between heat added and heat rejected increases (decreases) with increasing $\gamma_\circ(k_1)$. It can be concluded that the effect of $\gamma_\circ$ is more than that of k_1 on the power output and thermal efficiency. It should be noted here that both the heat added and the heat rejected by the working fluid decrease with increasing $\gamma_\circ$, and increase with the increase of k_1 (see Eqs. (2) and (3)).

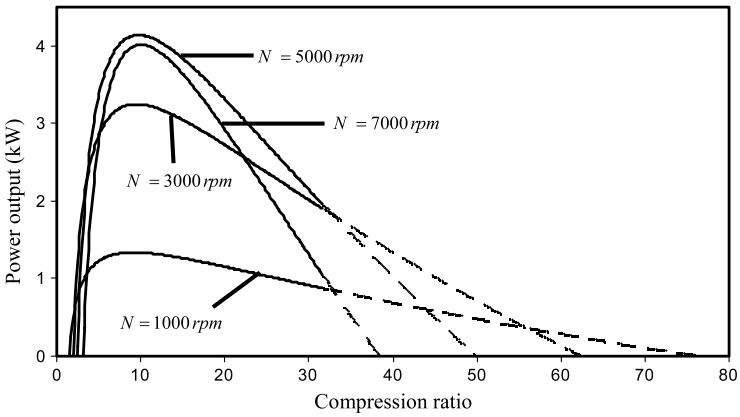

Fig. 6. Effect of N on the $P_{out} - r_c$ characteristic for $k_1 = 0.00008\ \mathrm{K}^{-1}$ and $\gamma_\circ = 1.4$.

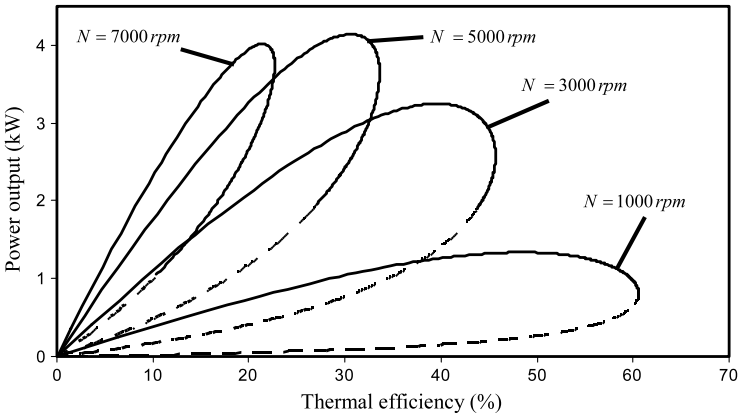

Fig. 7. Effect of N on the $P_{out} - \eta_{th}$ characteristic for $k_1 = 0.00008\ \mathrm{K}^{-1}$ and $\gamma_\circ = 1.4$.

Loop-shaped curves of power output versus thermal efficiency plots are depicted in Figs. 5 and 6. It is found that the power output at maximum thermal efficiency and the thermal efficiency at maximum power output decrease (increase) by about 8.4% (8.3%) and 2.2% (1.6%), respectively, when $\gamma_\circ(k_1)$ increases by 6.4% (80%). When comparing these results with results of Ref. [15], it is concluded that the linear variation of the specific heat ratio has a greater effect on the performance of the Miller cycle than that of specific heats.

Figs. 6–7 show the influence of the parameter N on the Miller cycle performance. It can be seen that the engine speed plays a significant role on the Miller cycle performance. The maximum power output increases with increasing engine speed up to about 5000 rpm where it reaches its peak value then starts to decline as the engine speed increases. The range of r_c in which the cycle can work normally remains constant with increase of engine speed. The optimal compression ratio corresponding to maximum power output point decreases with the increase of engine speed. It can also be concluded that, e.g. at the compression ratio of 11, the power output increases with the increase of engine speed and then decreases. This is consistent with the experimental results in the internal combustion engine [28,33]. The results also show that if the compression ratio is less than a certain value, the power output decreases with increasing engine speed, while if compression ratio exceeds a certain value, the power output first increases and then starts to decrease with increasing engine speed. With a further increase in compression ratio, the increase in engine speed results in decreasing the power output. Numerical calculation shows that for any same compression ratio, the smallest power output is for $N = 7000$ rpm when $r_c \leq 3.6$ or $r_c > 32.8$ and is for $N = 1000$ rpm when $3.6 < r_c \leq 32.8$ and also the largest power output is for $N = 1000$ rpm when $r_c \leq 2.2$ or $r_c > 55.9$, is for $N = 3000$ rpm when $2.2 < r_c \leq 3.6$ or $32.9 \leq r_c \leq 55.9$ and is for $N = 5000$ rpm when $3.6 < r_c < 32.9$. The influence of the engine speed on the power output versus thermal efficiency is displayed in Fig. 7. As can be seen from this figure, the power output versus thermal efficiency is a loop shaped one. It can be seen that the power output at maximum thermal efficiency improves with increasing engine speed from 1000 to around 5000 rpm. With the further increase in engine speed, the power output at maximum thermal efficiency decreases. It can also be seen that the thermal efficiency at maximum power decreases with the increase of engine speed from 1000 to 7000 rpm.

According to above analysis, it can be found that the effects of the engine speed and the specific heat ratio on the cycle performance are obvious, and they should be considered in practice cycle analysis in order to make the cycle model more close to the practice.

4. Conclusion

This study is aimed at investigating the effects of engine speed and variable specific heat ratio of the working fluid on the Miller cycle's performance. By using finite time thermodynamics theory, the characteristic curves of the power output versus compression ratio and the power output versus thermal efficiency are obtained. In the model, the nonlinear relation between the specific heats of working fluid and its temperature, the frictional loss computed according to the mean velocity of the piston, and heat transfer loss are considered. The results show that if the compression ratio is less than a certain value, the increase of the value of the specific heat ratio will increase the power output. In contrast, if the compression ratio exceeds a certain value, the increase of the value of the specific heat ratio will reduce the power output. It can be concluded that, e.g. at the compression ratio of 11, the power output decreases with a decrease of the value of specific heat ratio. This is consistent with the experimental results in the real internal combustion engine [28,34]. It should be noted here that the increase of EGR induction rate in internal combustion engines decreases the value of the specific heat ratio of the mixture (EGR and fresh air) in the cylinder. The results also show that if the compression ratio is less than a certain value, the power output decreases with increasing engine speed, while if compression ratio exceeds a certain value, the power output first increases and then starts to decrease with increasing engine speed. With a further increase in compression ratio, the increase in engine speed results in decreasing the power output. The results obtained from this research may be used with assurance to provide guidance for the analysis of the behavior and design of practical Miller engines.

Acknowledgments

The author would like to thank the Shahrekord University for the financial support. I would also like to thank the reviewers for valuable comments and suggestions.

References

[1] B. Andresen, P. Salamon, R.S. Berry, Thermodynamics in finite time, Phys. Today (1984) 62–70.
[2] L. Chen, J. Wang, F. Sun, Power density analysis and optimization of an irreversible closed intercooled regenerated Brayton cycle, Math. Comput. Modelling 48 (3–4) (2008) 527–540.
[3] R. Ebrahimi, Effects of mean piston speed, equivalence ratio and cylinder wall temperature on performance of an Atkinson engine, Math. Comput. Modelling 53 (5–6) (2011) 1289–1297.
[4] A. Parlak, The effect of heat transfer on performance of the diesel cycle and exergy of the exhaust gas stream in a LHR diesel engine at the optimum injection timing, Energy Conversion and Management 46 (2005) 167–179.
[5] C.G. Jesudason, Focus on the Clausius inequalities as a consequence of modeling thermodynamic systems as a series of open Carnot cycles, Math. Comput. Modelling 49 (2009) 835–842.
[6] R.H. Miller, Supercharging and internally cooling for high output, ASME Transactions 69 (4) (1947) 453–464.
[7] U. Kesgin, Efficiency improvement and NOx emission reduction potentials of two-stage turbocharged Miller cycle for stationary natural gas engines, International Journal of Energy Research 29 (3) (2005) 189–216.
[8] K. Hatamura, M. Hayakawa, T. Goto, M. Hitomi, A study of the improvement effect of Miller-cycle on mean effective pressure limit for high-pressure supercharged gasoline engines, JSAE Review 18 (1997) 101–106.
[9] Y. Fukuzawa, H. Shimoda, Y. Kakuhama, H. Endo, K. Tanaka, Development of high efficiency Miller cycle gas engine, Technical Review 38 (2001) 146–150. Mitsubishi Heavy Industries, Ltd..
[10] A. Al-Sarkhi, B.A. Akash, J.O. Jaber, M.S. Mohsen, E. Abu-Nada, Efficiency of Miller engine at maximum power density, International Communications in Heat and Mass Transfer 29 (8) (2002) 1159–1167.
[11] M. Sasaki, S. Araki, T. Miyata, T. Kawaji, Development of capacitor hybrid system for urban buses, JSAE Review 23 (2002) 451–457.
[12] C. Wu, P.V. Puzinauskas, J.S. Tsai, Performance analysis and optimization of a supercharged Miller cycle Otto engine, Applied Thermal Engineering 23 (2003) 511–521.
[13] Y. Ge, L. Chen, F. Sun, C. Wu, Effects of heat transfer and friction on the performance of an irreversible air-standard Miller cycle, International Communications in Heat and Mass Transfer 32 (8) (2005) 1045–1056.
[14] Y. Ge, L. Chen, F. Sun, C. Wu, Reciprocating heat-engine cycles, Applied Energy 81 (4) (2005) 397–408.
[15] Y. Ge, L. Chen, F. Sun, C. Wu, Effects of heat transfer and variable specific heats of working fluid on performance of a Miller cycle, International Journal of Ambient Energy 26 (4) (2005) 203–214.
[16] A. Al-Sarkhi, J.O. Jaber, S.D. Probert, Efficiency of a Miller engine, Applied Energy 83 (2006) 343–351.
[17] Y. Zhao, J. Chen, Performance analysis of an irreversible Miller heat engine and its optimum criteria, Applied Thermal Engineering 27 (2007) 2051–2058.
[18] A. Al-Sarkhi, I. Al-Hinti, E. Abu-Nada, et al., Performance evaluation of irreversible Miller engine under various specific heat models, International Communications in Heat and Mass Transfer 34 (7) (2007) 897–906.
[19] J.C. Lin, S.S. Hou, Performance analysis of an air-standard Miller cycle with considerations of heat loss as a percentage of fuel's energy, friction and variable specific heats of working fluid, International Journal of Thermal Sciences 47 (2008) 182–191.
[20] L. Chen, W. Zhang, F. Sun, Power, efficiency, entropy-generation rate and ecological optimisation for a class of generalised irreversible universal heat-engine cycles, Applied Energy 84 (2007) 512–525.
[21] J. Liu, J. Chen, Optimum performance analysis of a class of typical irreversible heat engines with temperature-dependent heat capacities of the working substance, International Journal of Ambient Energy 31 (2) (2010) 59–70.
[22] J.A. Gatowski, E.N. Balles, K.M. Chun, F. Nelson, J.A. Ekchian, F.B. Heywood, A heat release analysis of engine pressure data, in: SAE Paper 841359, 1984.
[23] M. Klein, A specific heat ratio model and compression ratio estimation, Department of Electrical Engineering, Ph.D. Thesis, Linkoping University, Sweden, 2004.
[24] M.F.J. Brunt, H. Rai, A.L. Emtage, The calculation of heat release energy from engine cylinder pressure data, in: SAE Paper 981052, 1998.
[25] M.A. Ceviz, I. Kaymaz, Temperature and air–fuel ratio dependent specific heat ratio functions for lean burned and unburned mixture, Energy Conversion and Management 46 (2005) 2387–2404.
[26] A. Maiboom, X. Tauzia, J.F. Hetet, Experimental study of various effects of exhaust gas recirculation (EGR) on combustion and emissions of an automotive direct injection diesel engine, Energy 33 (2008) 22–34.
[27] R. Ebrahimi, Effects of variable specific heat ratio of working fluid on performance of an endoreversible diesel cycle, Journal of Energy Institute 83 (1) (2010) 1–5.

[28] J.B. Heywood, Internal Combustion Engine Fundamentals, McGraw-Hill, New York, 1988.
[29] R. Ebrahimi, Effects of variable specific heat ratio on performance of an endoreversible Otto cycle, Acta Physica Polonica A 117 (6) (2010) 887–891.
[30] R. Ebrahimi, Performance analysis of a dual cycle engine with considerations of pressure ratio and cut-off ratio, Acta Physica Polonica A 118 (4) (2010) 534–539.
[31] L. Chen, Y. Ge, F. Sun, The performance of a Miller cycle with heat transfer, friction and variable specific heats of working fluid, Termotehnica 14 (2) (2010) 24–32.
[32] L. Chen, Y. Ge, F. Sun, et al. Finite time thermodynamic modeling and analysis for an irreversible Miller cycle, International Journal of Ambient Energy (in press).
[33] M. Mercier, Contribution to the study of the behavior of a spark ignition engine fueled with Groningen natural gas, Ph.D. Thesis Université de Valenciennes et du Hainaut-Cambrésis France, 2006 (in French).
[34] A. Hocine, Improvement of the warm-up phase of an automobile internal combustion engine by exhaust gas heat recovery and modified fuel injection parameters, Ph.D. Thesis, Université de Valenciennes et du Hainaut-Cambrésis, 2003 (in French).